

Importance of Charge Transfer and Polarization Effects for the Modeling of Uranyl–Cation Complexes

Lars Hemmingsen,^{*,†} Patricia Amara,[‡] Eric Ansoborlo,[§] and Martin J. Field^{*,‡}

Department of Mathematics and Physics, The Royal Veterinary and Agricultural University, Thorvaldsensvej 40, DK-1871 Frederiksberg C, Denmark, Laboratoire de Dynamique Moléculaire, Institut de Biologie Structurale—Jean-Pierre Ebel, CEA/CNRS 41, rue Jules Horowitz, F-38027 Grenoble Cedex 01, France, and Institut de Protection et de Sécurité Nucléaire, Département de Protection de la Santé de l'Homme et de Dosimétrie, Service de Dosimétrie, IPSN-BP 38, F-26701 Pierrelatte Cedex, France

Received: December 14, 1999; In Final Form: February 10, 2000

The structures, energies, and charges of uranyl cation complexes with water molecules, nitrate ion, and carbonate ions were determined using Hartree–Fock, second-order Möller–Plesset (MP2) perturbation theory, and density functional theory (DFT) ab initio quantum chemical methods. Reasonable agreement with experimentally determined structures was found. Significant polarization of the ligands as well as charge transfer to the uranyl ion was observed in the complexes. The dissociation energy curves for the complexes were also determined at the MP2 level of theory. Attempts to reproduce these curves with molecular mechanical models with fixed atomic point charges failed, showing that an appropriate force field for these systems must include polarization and charge-transfer effects.

1. Introduction

During the past decades the actinide elements have attracted intense experimental and theoretical interest.^{1–3} The reasons for this are, of course, that they are radioactive, chemically toxic, and of great importance for the nuclear-power industry. A major rationale for much actinide work has been that of detoxification after contamination due to accident or dumping. Thus, effort has gone into the identification of agents that promote the excretion of uranium,⁴ plutonium,⁵ and neptunium⁶ from the human body and into how to separate actinide ions from other ions in the management of nuclear waste.^{7,8}

Molecular modeling and theoretical simulation studies are potentially powerful approaches for tackling such problems and can be used, for example, to compute the association constant of different chelating agents to uranium or plutonium in solution. A few studies of this kind have appeared in the literature. They employed molecular mechanical (MM) force fields to determine the coordination geometry of various uranyl complexes and the free energies for association of the uranyl ion with water, NO₃[−], 18-crown-6, CMPO, and calix[6]arene^{6–9–14} A problem with the MM force fields used in these investigations, though, was that the charge distribution of each molecule was fixed, being represented by partial point charges on the atoms, and so no account was taken of electronic reorganization effects due to interactions between the ligands or between the ligands and the solvent. A more recent study attempted to estimate the magnitude of some of these effects by performing simulations of UO₂(NO₃)₂O=PR₃ (R = H, methyl or phenyl) 1:1 and 1:2 complexes and calculating the free-energy differences between two different states of the complexes—one in which the charge distribution was that of the complex itself and the other in which

it was that of the separated UO₂(NO₃)₂ and O=PR₃ species.¹⁵ Once again, however, effects such as polarization and charge transfer were partially neglected due to the fixed point charge representation of the charge distributions.

Our main interest in modeling uranyl and its complexes has been in the design of chelating compounds for the treatment of contamination and the detoxification of human serum. To perform such modeling, however, it is necessary to have a reasonable representation of the force field for the uranyl ion and its ligands. We have, therefore, undertaken a number of quantum chemical calculations to gain insight into the nature of the bonding in uranyl complexes and data for our parametrizations. Previous quantum mechanical studies on uranyl complexes have indicated that the bonding is primarily ionic.^{16,17}

In this paper, we focus on the uranyl ion, UO₂²⁺, and on the ligands H₂O, NO₃[−], and CO₃^{2−}. The uranyl ion is the most important species in the aqueous chemistry of uranium and is the predominant biological form of uranium in the blood and in tissue. The coordination chemistry of the uranyl ion has been investigated in several experimental studies, and a large number of structures (about a hundred) with these three ligands can be found in the Cambridge Structural Database (CSD).¹⁸ Furthermore, structural and thermochemical data also exist for the association of uranyl with NO₃[−] and CO₃^{2−} in solution.^{3,19,20} Nitrate is found in high concentrations in liquid solutions of nuclear waste²¹ and carbonate and bicarbonate are found in significant concentrations in many natural waters and are therefore of interest as complexing agents for uranyl in environmental chemistry.²² Recent theoretical studies of the uranyl ion have looked at its complexes with OH[−], H₂O, NO₃[−], CO₃^{2−}, SO₄^{2−} and O=PR₃ (R = H, methyl or phenyl).^{15,16,23,24}

The outline of this paper is as follows. Section 2 describes the methods we have used to study uranyl and its ligands, section 3 discusses the results we obtained, and section 4 concludes.

[†] The Royal Veterinary and Agricultural University.

[‡] Institut de Biologie Structurale—Jean-Pierre Ebel.

[§] Service de Dosimétrie.

2. Methods

The actinides present considerable challenges for quantum chemical techniques because they can have complicated bonding, potentially involving 5f, 6p, 6d, 7s, and 7p atomic orbitals, and because relativistic effects can be significant.^{17,25} For our study, we mostly employed the program package CADPAC,²⁶ although some of our calculations were done with GAUSSIAN 94.²⁷ Depending upon the system, we used either a restricted Hartree–Fock (HF) method, second-order Möller–Plesset perturbation theory (MP2) (all electrons active),²⁸ or density functional theory (DFT)²⁹ with the B3LYP functional.³⁰

Due to the large number of electrons that uranium has, it is usual to neglect the core electrons and replace them by a pseudopotential. In our study, the effect of the 78 core electrons of uranium was represented by the relativistic one-electron effective core potential (ECP) of Hay (up to and including 4f and 5d electrons), and a [3s3p2d2f] contracted Gaussian basis set was used for the remaining 14 electrons.²⁶ Both the ECP and the corresponding basis set were derived for use with HF calculations. However, previous work has shown that it is feasible to use them with DFT methods.^{31,32} Likewise, calculations on transition metal complexes with equivalent basis set/ECP combinations have given good results,^{32,33} and so we assume that this is also a valid approach in our work. For the other atoms, different basis sets were employed, including 6-31G(d), 6-31G(2dp) (a 6-31G basis with two polarization functions and a set of diffuse sp functions), double- ζ (DZ) and double- ζ with polarization (DZP) sets.²⁸ We should note that, in the rest of the paper, we will only explicitly define the basis set on the non-uranium atoms, it being understood that the basis set/ECP combination discussed above is always used for uranium. In all calculations, d- and f-functions were taken to have 6 and 10 Cartesian components, respectively.

Two distinct types of calculation were done. The first consisted of geometry optimizations of the uranyl cation and some of its complexes. The calculations were performed by optimizing all the available geometrical degrees of freedom, without symmetry constraints, and the optimizations were taken to have converged when the rms gradient for the complex was less than 10^{-4} hartrees bohr⁻¹.

The second set of calculations were profiles for the dissociation energy of the uranyl ion and the ligands H₂O, NO₃⁻, and CO₃²⁻. In these calculations, the internal geometry of the molecules was held fixed, and only the distances between the uranyl ion and ligands were altered. The uranyl cation is linear and we chose a U–O bond length of 1.761 Å which is the value derived from experimentally determined structures in the CSD (see next section). The structures of NO₃⁻ and CO₃²⁻ were optimized at the MP2 level using the AUG-cc-pVDZ basis in GAUSSIAN 94,²⁷ giving N–O and C–O bond lengths of 1.2699 and 1.3152 Å, respectively. These values correspond well to the experimentally determined bond lengths for these ions in crystalline systems which are found to be in the ranges 1.22–1.27 and 1.27–1.31 Å, respectively.³⁴ The structure of H₂O was taken from reference 35.

For both sets of calculations, charge analyses were performed and binding energies were calculated. The charge analyses were done either by a Mulliken procedure in CADPAC or by using the CHELPG algorithm in GAUSSIAN. The binding energy of a complex AB_n was estimated as $\Delta E_{AB_n} = E_{AB_n} - E_A - nE_B$ where E_X is the energy of species X. When determining the dissociation energy curves, the binding energies were corrected for basis set superposition error (BSSE) using the counterpoise method.³⁶

TABLE 1: Results of Optimizing the Uranyl Cation with Different Methods and Basis Sets^a

method/basis set	U–O/Å	energy/hartrees	q_U/e	q_O/e
B3LYP/DZ	1.731	–201.1150	1.92	0.04
B3LYP/DZP	1.708	–201.1621	2.15	–0.08
HF/DZ	1.666	–199.6631	2.14	–0.07
HF/DZP	1.648	–199.7373	2.42	–0.21
MP2/DZ	1.783	–200.3652	1.84	0.08
MP2/DZP	1.747	–200.5345	2.07	–0.04

^a q_U and q_O are the Mulliken charges of the atoms U and O, respectively.

3. Results and Discussion

3.1. The Uranyl Cation. The structure of the uranyl cation was optimized at the HF, MP2, and B3LYP levels with both DZ and DZP basis sets on the oxygens. The results are given in Table 1. It can be seen that the optimized U–O bond lengths deviate quite substantially from each other and range from 1.65 to 1.78 Å, depending on the type of calculation. The Hartree–Fock method gives the shortest bond lengths, and inclusion of polarization functions on the ligands systematically decreases the bond length by 0.02–0.04 Å. This behavior has also been found by others.^{16,17,24}

It is interesting to compare these results with U–O distances determined experimentally. Although, our calculations are in the gas phase, the most comprehensive experimental source of structural data is derived from X-ray crystallographic studies and stored in the CSD. Here there are about a thousand structures that contain uranium. From these we selected complexes in which there was a uranyl ion coordinating to either carbonate, phosphate, sulfate, nitrate, or water. As a further criterion, we only accepted complexes with at least two coordinating water molecules if none of the other ligands were present. This left us with 76 structures in total from which we found that the mean U–O distance was 1.761 ± 0.039 Å with a minimum of 1.6795 Å and a maximum of 1.9489 Å. The distribution of distances was very strongly peaked around the mean value with frequencies of 1.65–1.70, 8; 1.70–1.75, 37; 1.75–1.80, 94; 1.80–1.85, 7; 1.85–1.90, 3; 1.90–1.95, 3. It should be noted that we made no attempt to take into account the resolution of each structure in deriving these results.

Table 1 also shows the Mulliken charges for the uranium and oxygen atoms obtained for each of the optimized complexes. As with the bond lengths, there is a significant variation depending upon the method and basis set, with the trend that a shorter bond length gives a higher charge on uranium. As Mulliken charges do not seem to model properly the charge distribution in the U–O bond,¹⁶ the charges on the atoms of the uranyl ion were also obtained from a fit to the electrostatic potential, derived from a HF/DZ calculation, using the CHELPG procedure.²⁷ The fitting requires atomic radii for the construction of the surface where the electrostatic potential is calculated, but as there is no default radius for uranium in GAUSSIAN, we tried values in the range 1.0–2.5 Å. The results are shown in Table 2 and indicate that there is only a small variation of 0.15 e in the charge of the uranium as its radius is increased from 1.5 to 2.5 Å, but there is a significant increase when the radius is decreased to 1.0 Å. In addition to the fits done to the electrostatic potential, the table also shows the results of a fit done to reproduce some of the lower order multipole moments of the uranyl cation.³⁷ The charges obtained are similar to those resulting from a fit to the electrostatic potential with a large uranium radius. As a final test, we investigated the dependence of the atomic charges as a function of the U–O bond length

TABLE 2: Atomic Charges for the Uranyl Cation Obtained by Fitting an Atom-Centered Point Charge Representation of the Cation's Charge Distribution to the Electrostatic Potential at the Molecule's Surface Calculated at the HF/DZ Level of Theory

U–O/Å	U radius/Å	U and O charges/e
1.761	1.0	3.330/–0.665
1.761	1.5	3.010/–0.505
1.761	2.0	2.918/–0.459
1.761	2.5	2.858/–0.426
1.761 ^a		2.832 ± 0.13/–0.416 ± 0.09
1.650	1.5	2.958/–0.479
1.900	1.5	3.058/–0.529

^a This fit was done to reproduce the quadrupole, octupole, and hexadecapole moments of the cation (with statistical weights of 1.0, 0.11115, and 0.01235, respectively) and not the electrostatic potential.

TABLE 3: Structures and Relative Energies of Uranyl–Water Complexes Obtained from Geometry Optimizations at the B3LYP/DZ Level of Theory^a

<i>n</i> ^a	U–O _{UO₂²⁺} /Å	O–U–O _{UO₂²⁺} /deg	U–O _{H₂O} /Å	ΔE/kJ mol ^{–1}
0	1.731	180.0		0
1	1.744	179.9	2.338	–341
2	1.755	180.0	2.381	–638
3	1.766	180.0	2.402	–908
4	1.776	180.0	2.430	–1129
5	1.781	180.0	2.488	–1260
5 ^b	1.720	180.0	2.503	–1218
5 ^c	1.71	180	2.45	
5 ^d	1.702	180	2.421	

^a Results are shown for complexes with *n* = 0–5 water molecules. ^b An additional result at the HF/DZ level of theory. ^c From an experiment in the solid state. ^d From an experiment in solution.³⁸

and found that the variation is not large, the charge on the uranium decreasing (increasing) slightly as the bond length decreases (increases).

As a result of the above analysis, in the rest of the paper and in our MM model of the uranyl cation, we assign charges of 2.9 and –0.45 e to the uranium and oxygen atoms, respectively. These values compare with those previously published in the literature of 2.8/–0.4¹⁶ and 2.5/–0.25 e.¹¹

3.2. Geometry Optimizations of Uranyl–Water and Uranyl–Carbonate Complexes. Geometry optimizations were performed of uranyl–water complexes UO₂(H₂O)_{*n*}²⁺ with *n* varying from 1 to 5 and the uranyl–carbonate complex UO₂(CO₃)₃^{4–}. The optimizations of the water complexes were done with a B3LYP/DZ method while those of the carbonate complexes were done at both the HF/DZ and B3LYP/DZ levels of theory.

The structures and relative energies for the optimized uranyl–water complexes are presented in Table 3. Similar calculations on uranyl–water complexes with from 4 to 6 water molecules have been reported by Spencer et al.²⁴ The oxygens of all the water molecules are found in the equatorial plane with the hydrogen atoms positioned perpendicular to this plane. The only complex in which the uranyl ion is expected to be bent is UO₂(H₂O)₂²⁺, and this is indeed the case, but only by a very small amount (an angle of 179.9°). The U–O_{H₂O} bond length increases by about 0.03 Å for each additional water molecule added, whereas the U–O_{UO₂} bond length increases by about 0.01 Å for each additional water.

The binding energies for the complexes were determined as described in section 2. We have introduced neither BSSE nor zero-point energy (ZPE) corrections for these complexes, because we are only interested in an estimate of the binding

TABLE 4: A Mulliken Analysis of the Charges on the Atoms in the Uranyl–Water Complexes^a

<i>n</i>	<i>q</i> _U	<i>q</i> _{O(UO₂²⁺)}	<i>q</i> _{UO₂²⁺}	<i>q</i> _{O(H₂O)}	<i>q</i> _{H(H₂O)}	<i>q</i> _{H₂O}
0	1.92	0.04	2.00	–0.69	0.35	0.00
1	1.80	–0.04	1.72	–0.77	0.52	0.27
2	1.72	–0.10	1.52	–0.78	0.51	0.24
3	1.67	–0.15	1.37	–0.79	0.50	0.21
4	1.65	–0.20	1.25	–0.78	0.49	0.20
5	1.66	–0.22	1.22	–0.78	0.47	0.16

^a Results are shown for complexes with 1–5 water molecules. The entries corresponding to *n* = 0 refer to the species at infinite separation. Charges are in units of the fundamental charge *e*.

energies, not quantitative values. These would, in any case, be hard to get with the presently available basis sets for uranium. The energy of the isolated water was determined at the reference geometry of reference 35 and that of the uranyl ion at the optimized geometry appropriate for the method and basis set being used to study the complex. The energy values, which are listed in the last column of Table 3, show that the binding is very strong. This is in agreement with the findings of Spencer et al., who also note that the binding is likely to be significantly weakened in solution.²⁴ These latter workers also determined BSSE and ZPE corrections and showed that they amounted to only a few percent in the total binding energies.

It is possible to compare the B3LYP structure for the complex UO₂(H₂O)₅²⁺ with those obtained experimentally in solution and in the crystal.^{38,39} These are shown in Table 3 along with the results of an optimization at the HF level of theory. Both the HF and B3LYP calculations overestimate the U–O distances, those between the uranium and the water oxygens by 0.04–0.08 Å, respectively, and those between the uranium and the uranyl oxygen by 0.01–0.08 Å, respectively. These differences, although not large, could be due to the fact that the calculations are performed for the complexes in gas phase as opposed to the condensed phase or due to limitations in the basis set. Indeed, it can be seen from Table 1 that the U–O bond length in UO₂²⁺ decreases by up to 0.03 Å on going from a DZ to a DZP basis set.

The results of a Mulliken charge analysis for the uranyl–water complexes are shown in Table 4. The charge on the uranyl ion decreases for each additional water molecule added, by about 0.27 e for the first water and by about 0.16 e per water in the complex with five water molecules. This clearly demonstrates that charge transfer is significant even with an uncharged ligand. The added charge is approximately equally distributed between the uranium and the oxygens of UO₂²⁺. The water molecules are clearly polarized by the uranyl ion, as can be seen by comparing the Mulliken charges of gas phase water (the first line in Table 4) with complexed water. This effect weakens as the coordination number increases, probably because the charge of the uranyl is decreased by charge transfer from the water molecules. Interestingly, the charges on the water oxygens are almost constant, independent of the number of coordinating water molecules.

The structure of the complex UO₂(CO₃)₃^{4–} was optimized at the HF/DZ and the B3LYP/DZ levels of theory. The results are compared with the experimental values in Table 5. The agreement between the calculated and experimental values is reasonable, although the calculations overestimate the U–O_{CO₃} bond length by about 0.12 Å and the C–O bond length for the non-coordinating oxygen by about 0.05 Å. Again these differences may be due to the fact that the calculations are performed in the gas phase or because of deficiencies in the theoretical approach. The binding energy for the complex is found to be

TABLE 5: Structures and Relative Energies of the $\text{UO}_2(\text{CO}_3)_3^{4-}$ Complex Obtained from Geometry Optimizations at the HF/DZ and B3LYP/DZ Levels of Theory^a

method	U–O _{UO₂} /Å	O–U–O _{UO₂} /deg	U–O _{CO₃} /Å	C–O _c ^a /Å	C–O _u ^a /Å	O–C–O/deg	$\Delta E/\text{kJ mol}^{-1}$
B3LYP/DZ	1.848	180.0	2.576	1.344	1.307	112.7	–2833
HF/DZ	1.765	180.0	2.573	1.317	1.283	112.1	–2662
experiment	1.79 ± 0.01	180	2.45 ± 0.01	1.33 ± 0.02	1.24 ± 0.03	115 ± 2	

^a The O_c type corresponds to the two oxygen atoms per carbonate that coordinate the uranium atom, whereas the O_u type is the uncoordinated oxygen. The experimental data are from ref 43.

TABLE 6: A Mulliken Analysis of the Charges on the Atoms in the $\text{UO}_2(\text{CO}_3)_3^{4-}$ Complex and in the Separated Uranyl and Carbonate Ions^a

method	q_U	$q_{O(\text{UO}_2)}$	q_{UO_2}	$q_{O_c}^b$	$q_{O_u}^b$	$q_{C(\text{CO}_3)}$	q_{CO_3}
B3LYP/DZ gas phase	1.92	0.04	2.00	–0.65	–0.65	–0.04	–2.00
B3LYP/DZ complex	1.33	–0.50	0.33	–0.51	–0.58	0.16	–1.44
HF/DZ gas phase	2.14	–0.07	2.00	–0.82	–0.82	0.45	–2.00
HF/DZ complex	2.06	–0.55	0.96	–0.74	–0.73	0.55	–1.66

^a Charges are in units of the fundamental charge *e*. ^b O_c and O_u refer to the coordinated and uncoordinated oxygens of the carbonate, respectively.

much larger than that for the uranyl–water complexes with a value of about 2600 kJ mol^{–1}. In a simplified model, this can be explained by the fact that the charge–charge attraction driving the uranyl–carbonate complexation is stronger than the charge–dipole attraction of the uranyl–water complexes.

In Table 6, the Mulliken charges of the ions in gas phase and in the complex are presented. There is a very large charge-transfer effect from the carbonates to the uranyl. Both the HF and B3LYP calculations predict similar changes in the carbonate carbon, carbonate oxygen, and uranyl oxygen atom charges on complexation. They differ, however, on how the charge of the uranium changes. The change is small (~ -0.1 e) in the HF calculation but much larger with B3LYP (~ -0.6 e). It is worth remarking, however, that at both levels of theory the charge of the uranyl lessens substantially and much more so than it does in its complexes with water. In contrast to the case of the uranyl–water complexes, the calculations indicate that there is little polarization of the carbonate ions, possibly because the uranyl ion has been neutralized to a large extent.

A comparison of the general details of the complexes' structures that we optimized here with the structures that we selected from the CSD shows good agreement—the coordinating ligand atoms tend to be positioned in the plane perpendicular to the O–U–O axis, and in this plane, the coordinating atoms of different ligands are positioned so that they are as far apart from each other as possible. Thus, the structures of the complexes can be considered to be due to a compromise between the electrostatic charge–charge or charge–dipole attraction between uranyl and ligand and the ligand–ligand repulsions.

3.3. Uranyl–Ligand Dissociation Energy Curves. To gain further insight into the nature of the bonding in the uranyl complexes and more data for the generation of a reasonable uranyl MM force field, we determined the dissociation energy curves for the uranyl ion and water, nitrate, and carbonate ligands. Schematics of the geometries of the complexes that we used in these calculations are shown in Figure 1.

To estimate the MM electrostatic interaction energy between the uranyl ion and its ligands water, nitrate and carbonate, we had to derive atomic point charge models for the ligands. For nitrate and carbonate we obtained the charges by performing HF calculations with the 6-31G(d) basis set using the CHELPG algorithm. This gave charges of 1.010 and –0.670 e for the nitrogen and the oxygens of the nitrate ion and 1.198 and –1.066 e for the carbon and the oxygens of the carbonate ion, respectively. Repeating the calculations at the MP2 level with the same basis set elicited variations in the charges of up to 0.07 e per atom. It is common practice⁴⁰ when deriving MM

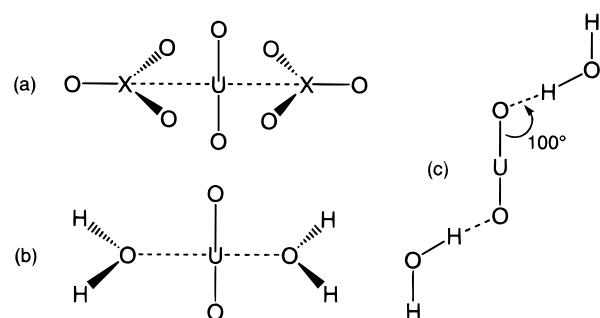


Figure 1. Schematics of the geometries of the uranyl cation complexes used for the calculation of the interaction energy curves: (a) the carbonate and nitrate complexes; (b) the water complex, equatorial approach; (c) the water complex, axial approach.

force fields to use HF/6-31G(d) CHELPG-derived charges because, in general, they give a dipole moment that is too large (although here neither of the ions have a dipole moment). This overestimation is assumed to make up for the lack of polarizability upon solvation.

For water we used a different approach and chose two different charge models. The first we obtained by fitting the charges to reproduce the dipole moment of the water molecule in a vacuum, 1.85 D. For our reference geometry this gave charges of –0.6574 and +0.3287 e on the oxygen and hydrogens, respectively. The second set of charges, –0.834 e on the oxygen and +0.417 e on the hydrogens, we took from the TIP3P model of water that is often used in MM simulations⁴¹ and which gives a dipole moment for the water molecule of 2.31 D.

The curves of the interaction energies between the uranyl ion and two water molecules, between the uranyl and two nitrates, and between the uranyl ion and two carbonates are shown in Figures 2, 3, and 4, respectively. Initially we tried doing these calculations with a B3LYP/6-31G(2dp) level of theory but we had severe convergence problems in the carbonate case and so switched to a MP2/6-31G(2dp) model. The calculated curves were corrected for BSSE because we wanted to have data of sufficient quality to use for parametrization of an MM force field for these systems.

Figures 2–4 also show the electrostatic interaction energy curves calculated with the point charge models that we derived for the uranyl ion and its ligands. All of the curves agree well with the MP2 results at intermediate and long distances but, except for the TIP3P charge model of water, fail to reproduce the depth of the well at the minima. We have attempted to model

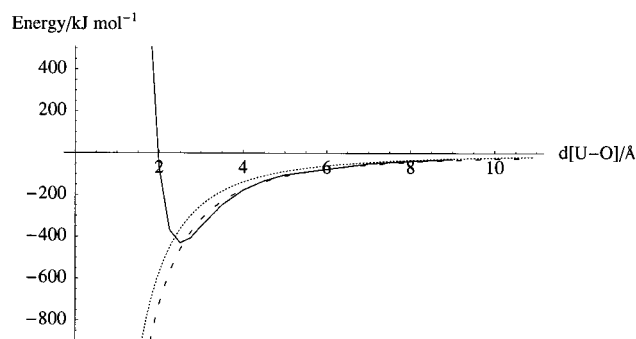


Figure 2. Interaction energy curves for the uranyl ion and two water molecules as a function of the uranium–water oxygen distances. The solid line is the curve of MP2/6-31G(2dp) energies, the dotted line is the MM electrostatic energy calculated using the vacuum charge model for water and the dashed line is the MM energy obtained with the TIP3P water model. The water molecules were approached in the equatorial plane of the uranyl ion from opposite sides of the uranium.

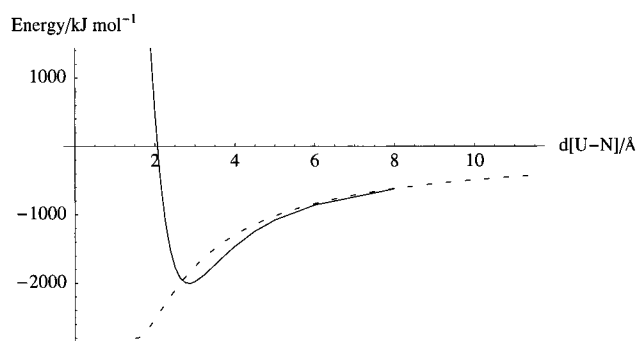


Figure 3. Interaction energy curves for the uranyl ion and two nitrate ions as a function of the uranium–nitrogen distances. The solid line is the curve of MP2/6-31G(2dp) energies, whereas the dashed line is the curve calculated using the MM electrostatic model. The nitrate ions were approached in the equatorial plane of the uranyl ion from opposite sides of the uranium.

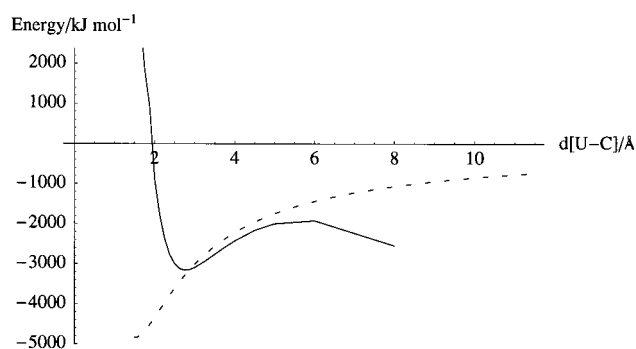


Figure 4. Interaction energy curves for the uranyl ion and two carbonate ions as a function of the uranium–carbonate oxygen distances. The solid line is the curve of MP2/6-31G(2dp) energies, whereas the dashed line is the curve calculated using the MM electrostatic model. The carbonate ions were approached in the equatorial plane of the uranyl ion from opposite sides of the uranium.

this extra deepening in our MM force field with suitably parametrized Lennard–Jones terms but it is just not possible to do so and maintain chemically valid values for the Lennard–Jones interaction parameters. Even if the point charges as well as the Lennard–Jones interaction parameters are varied within reasonable limits, the MM energies cannot reproduce the QM energies. This result implies that polarization and charge transfer effects are important in the binding of uranyl complexes and need to be included to have a useful model of uranyl–ligand interactions. It is interesting to note that the electrostatic energies

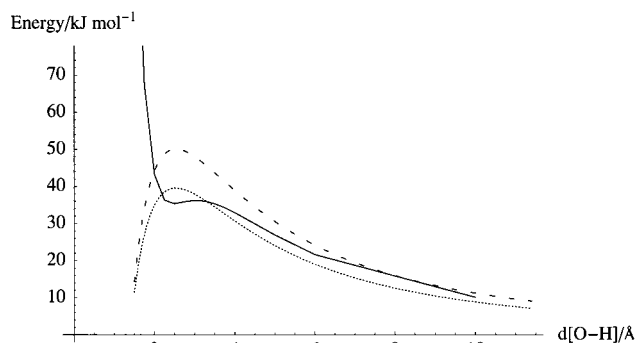


Figure 5. Interaction energy curves for the uranyl ion and two water molecules as a function of the uranyl oxygen–water hydrogen distances. The solid line is the curve of MP2/6-31G(2dp) energies, the dotted line is the MM electrostatic energy calculated using the vacuum charge model for water, and the dashed line is the MM energy obtained with the TIP3P water model. The water molecules were approached along the axis of the uranyl ion such that the angle subtended by the uranium, the uranyl oxygen, and the approaching water hydrogen had a value of 100°.

determined using the TIP3P charge model of water do give fair agreement with the MP2 energies, even at the minimum. The charges in the TIP3P model were, however, parametrized to reproduce the liquid-state properties of water and so implicitly take account of polarization effects through the enhanced value of the water dipole moment that they give. As noted above, the charges assigned to the atoms in NO_3^- and CO_3^{2-} are similarly expected to take into account (some of the) polarization effects, but even so the fixed point charge model does not reproduce the MP2 energies well for these systems.

As is clear from Figure 4, we were unable to dissociate the uranyl–carbonate complex to the species UO_2^{2+} and CO_3^{2-} . This is probably due to the fact that the highest occupied orbitals of CO_3^{2-} in gas phase have positive energies with the methods and basis sets used. The ions do, however, have the correct character up to a distance of about 5 Å, as judged by the Mulliken charges and the form of the curve in Figure 4. The Mulliken charges of the uranyl ion, water molecule and nitrate ion in $\text{UO}_2(\text{H}_2\text{O})_2^{2+}$ and $\text{UO}_2(\text{NO}_3)_2$ were also determined and found to have the appropriate values of +2, 0, and –1 e, respectively, at long distances.

For a final interaction energy curve, we determined the energies as the hydrogens of the two water molecules approach the uranyl ion along its axis. We did this because it has been suggested that improved uranyl–chelating agents can be designed by including at least one hydrogen-bond donor for interaction with the uranyl oxo groups.⁴² To determine the most favorable geometry for approaching the water molecules, we did calculations with values of the uranium–uranyl oxygen–water hydrogen angle ranging from 60° to 180° and chose the value, in this case 100°, which gave the lowest absolute energy. The oxygens of the water molecules point away from the uranium, and the water molecules themselves are in a trans-configuration with respect to each other.

The interaction energy curve is shown in Figure 5 and was calculated with an MP2/6-31G(2dp) level of theory. It is clear that the curve is essentially repulsive and is probably due to the fact that the water dipole is in the wrong orientation with respect to the net positive charge of the uranyl ion. This explanation is supported by the similar behavior of the curves of the MM electrostatic energies and suggests that the possibility of a hydrogen bond may depend on the type of ligands in the equatorial plane. If they are negatively charged, thereby producing a zero (e.g. $\text{UO}_2(\text{NO}_3)_2(\text{H}_2\text{O})_2$) or even a net negative charge

(e.g. $\text{UO}_2(\text{CO}_3)_3^{4-}$), hydrogen bonding may be facilitated, but if they are neutral, hydrogen bonding may be inhibited. In addition, ligands, such as carbonate, that promote a large charge transfer to the oxygens of the uranyl ion may also enhance hydrogen bonding. Finally, it is worth remarking that the MM energies obtained using the vacuum charge model of water agree better with the ab initio energies than those of the TIP3P charge model, indicating that polarization effects are less important in the uranyl–water interaction when the water molecules approach in an axial direction. Consequently, a single fixed point charge water model cannot appropriately account for the interactions for different configurations of uranyl–water complexes. TIP3P is the best of the two models for water molecules in the equatorial plane, whereas the vacuum water model is best for axially positioned water molecules.

4. Conclusions

In this paper we have examined some complexes of the uranyl ion UO_2^{2+} with the ligands water, nitrate, and carbonate using quantum chemical techniques. Our aim in doing this work has been to understand the interactions between the uranyl and its ligands so that we can parametrize a MM force field for these systems that can be used in molecular dynamics simulations.

The major point to have emerged from this work is that it is crucial to take into account charge transfer and polarization effects when attempting to study complex formation. This can be seen both from an analysis of the charges of the atoms in the complexes when compared to those in the isolated molecules and from the interaction energy curves. In previous work on uranyl complexes that used MM force fields,^{9–13,15} these effects were neglected, and it may be for this reason, for example, that a rather small charge had to be assigned to the uranium ion in uranyl¹¹ in order to get the correct free energy of solvation relative to Sr^{2+} . It is perhaps worth emphasizing that although the short-range interactions are not well-described by a purely MM model, the long-range interactions are fitted well by the electrostatic part of the MM energy.

To us it is clear that it is necessary to go beyond a standard MM force field if reasonable simulations of these systems in solution are to be performed. There are a number of approaches that can be envisaged. One possible way is to treat the complexes with a quantum mechanical potential directly, either in a fully ab initio simulation or as part of a hybrid potential,⁴⁴ but these methods are expensive. Another way, and the route we favor, is to employ an enhanced MM potential that includes charge transfer and polarization. While a substantial amount of work has been done to include polarization effects in MM force fields, less seems to have been done for charge transfer. Fortunately there is a method, the chemical potential equilibration (CPE) or fluctuating charge model,⁴⁵ that describes both effects and it is this that we intend to employ in our simulations. We are currently parametrizing a force field for some simple molecules that includes CPE and will report our results in due course.⁴⁶

Acknowledgment. We are grateful for the help of Ulf Ryde and Mats Olsson who calculated the charges on the uranyl ion in a vacuum. We would also like to thank the Danish Natural Science Research Council (L.H.), the Institut de Biologie Structurale – Jean-Pierre Ebel, the Commissariat à l’Énergie Atomique and the Centre National de la Recherche Scientifique (P.A., M.J.F.) for support of this work.

References and Notes

(1) Katz, J.; Seaborg, G. T.; Morss, L. R. *The Chemistry of the Actinide Elements*; Chapman and Hall: London, 1986.

- (2) *Handbook on the Physics and Chemistry of the Actinides*; Freeman, A. J., Keller, C., Eds.; Elsevier Science Publishers: Amsterdam, B.V. 1986.
- (3) Grenthe, I.; Fuger, J.; Konigs, R. J. M.; Lemire, R. J.; Muller, A. B.; Nguyen-Trung, C.; Wanner, H. *Chemical Thermodynamics of Uranium*; Elsevier Science Publishing Company, Inc.: North-Holland, 1992.
- (4) Henge-Napoli, M. H.; Ansoborlo, E.; Chazel, V.; Houpert, P.; Paquet, F.; Gourmelon, P. *Intl. J. Radiat. Biol.* **1999**, *75*, 1473.
- (5) Paquet, F.; Grillon, G.; Rateau, G.; Poncy, J. L.; Fritsch, P.; Burgada, R.; Bailly, T.; Raymond, K. N.; Durbin, P. W. *Intl. J. Radiat. Biol.* **1995**, *68*, 663.
- (6) Paquet, F.; Metivier, H.; Poncy, J. L.; Burgada, R.; Bailly, T. *Intl. J. Radiat. Biol.* **1997**, *71*, 613.
- (7) Rozen, A. M. *J. Radioanal. Nucl. Chem.* **1990**, *143*, 337.
- (8) Cecile, L.; Casarici, M.; Pietrelli, L. *New separation chemistry techniques for radioactive waste and other specific applications*; Commission of the European Communities, Elsevier Applied Science: New York, 1991.
- (9) Guilbaud, P.; Wipff, G. *J. Mol. Recognit. Inclusion Phenom.* **1993**, *16*, 169.
- (10) Guilbaud, P.; Wipff, G. *J. Phys. Chem.* **1993**, *97*, 5685.
- (11) Guilbaud, P.; Wipff, G. *J. Mol. Struct. THEOCHEM* **1996**, *366*, 55.
- (12) Guilbaud, P.; Wipff, G. *New J. Chem.* **1996**, *20*, 631.
- (13) Muzet, N.; Wipff, G.; Casnati, A.; Domiano, L.; Ungaro, R.; Ugozzoli, F. *J. Chem. Soc., Perkin Trans.* **1996**, *6*, 1065.
- (14) Vallet, V.; Maron, L.; Schimmelpfennig, B.; Leininger, T.; Teichtel, C.; Gropen, O.; Grenthe, I.; Wahlgren, U. *J. Phys. Chem. A* **1999**, *103*, 9285.
- (15) Hutschka, F.; Dedieu, A.; Troxler, L.; Wipff, G. *J. Phys. Chem. A* **1998**, *102*, 3773.
- (16) Craw, S.; Vincent, M. A.; Hillier, I. H.; Wallwork, A. L. *J. Phys. Chem.* **1995**, *99*, 10181.
- (17) Pyykkö, P.; Li, J.; Runeberg, N. *J. Phys. Chem.* **1994**, *98*, 4809.
- (18) Allen, F. H.; Kennard, O. *Chemical Design Automation News* **1993**, *8*, 31.
- (19) Bányai, I.; Glaser, J.; Micskei, K.; Tóth, I.; Zékány, L. *Inorg. Chem.* **1995**, *34*, 3785.
- (20) Allen, P. G.; Bucher, J. J.; Clark, D. L.; Edelstein, N. M.; Ekberg, S. A.; Gohdes, J. W.; Hudson, E. A.; Kaltsoyannis, N.; Lukens, W. W.; Neu, M. P.; Palmer, P. D.; Reich, T.; Shuh, D. K.; Tait, C. D.; Zwick, B. D. *Inorg. Chem.* **1995**, *34*, 4797.
- (21) Choppin, G. R.; Nach, K. L. *Radiochim. Acta* **1995**, *70/71*, 225.
- (22) Clark, D. L.; Hobart, D. E.; Neu, M. P. *Chem. Rev.* **1995**, *95*, 25.
- (23) Schreckenbach, G.; Hay, J. P.; Martin, R. L. *Inorg. Chem.* **1998**, *37*, 4442.
- (24) Spencer, S.; Gagliardi, L.; Handy, N. C.; Ioannou, A. G.; Skylaris, C.-K.; Willetts, A.; Simper, A. M. *J. Phys. Chem. A* **1999**, *103*, 1831.
- (25) Pepper, M.; Bursten, B. E. *Chem. Rev.* **1991**, *91*, 719.
- (26) *The Cambridge Analytic Derivatives Package Issue 6, Cambridge 1995*. A suite of quantum chemistry programs developed by R. D. Amos with contributions from I. L. Alberts, J. S. Andrews, S. M. Colwell, N. C. Handy, D. Jayatilaka, P. J. Knowles, R. Kobayashi, K. E. Laidig, G. Laming, A. M. Lee, P. E. Maslen, C. W. Murray, J. E. Rice, E. D. Simandiras, A. J. Stone, M.-D. Su, and D. J. Tozer.
- (27) Frisch, A. M.; Trucks, G. W.; Schlegel, H. B.; Gill, P. M. W.; Johnson, B. G.; Robb, M. A.; Cheeseman, J. R.; Keith, G. A.; Petersson, G. A.; Montgomery, J. A.; Raghavachari, K.; Al-Laham, M. A.; Zakrzewski, V. G.; Ortiz, J. V.; Foresman, J. B.; Cioslowski, J.; Stefanov, B.; Nanayakkara, A.; Challacombe, M.; Peng, C. Y.; Ayala, P. Y.; Chen, W.; Wong, M. W.; Andres, J. L.; Replogle, E. S.; Gomperts, R.; Martin, R. L.; Fox, D. J.; Binkley, J. S.; Defrees, D. J.; Baker, J.; Stewart, J. J. P.; Head-Gordon, M.; Gonzales, C.; Pople, J. A. *Gaussian 94 (Revision D.1 and D.4)*; Gaussian, Inc.: Pittsburgh, PA, 1995.
- (28) Hehre, W. J.; Radom, L.; Schleyer, P. v. R.; Pople, J. A. *Ab Initio Molecular Orbital Theory*; J. Wiley & Sons: New York, 1986.
- (29) Parr, R. G.; Yang, W. *Density-Functional Theory of Atoms and Molecules*; Clarendon Press: Oxford, 1989.
- (30) Becke, A. D. *J. Chem. Phys.* **1993**, *98*, 1372 and 5648.
- (31) Russo, T. V.; Martin, R. L.; Hay, P. J. *J. Phys. Chem.* **1995**, *99*, 17085.
- (32) Van Wüllen, C. *Int. J. Quantum Chem.* **1996**, *58*, 147.
- (33) Kaupp, M.; Malkin, V. G.; Malkina, O. L.; Salahub, D. R. *Chem. Phys. Lett.* **1995**, *235*, 382.
- (34) Radom, L. *Aust. J. Chem.* **1976**, *29*, 1635.
- (35) Benedict, W. S.; Plyler, K. *J. Chem. Phys.* **1956**, *24*, 1139.
- (36) Schwenke, D. W.; Truhlar, D. G. *J. Chem. Phys.* **1985**, *82*, 2418.
- (37) Sigfridsson E.; Ryde, U. *J. Comput. Chem.* **1998**, *19*, 377.
- (38) Åberg, M.; Ferri, D.; Glaser, J.; Grenthe, I. *Inorg. Chem.* **1983**, *22*, 3986.
- (39) Alcock, N. W.; Esperâs, S. *J. Chem. Soc., Dalton Trans.* **1977**, *1*, 893.

(40) Carlson, H. A.; Nguyen, T. B.; Orozco, M.; Jorgensen, W. L. *J. Comput. Chem.* **1993**, *14*, 1240.

(41) Jorgensen, W. L.; Chandrasekar, J.; Madura, J. D.; Impey, R. W.; Klein, M. L. *J. Chem. Phys.* **1983**, *79*, 926.

(42) Franczyk, T. S.; Czerwinski, K. R.; Raymond, K. N. *J. Am. Chem. Soc.* **1992**, *114*, 8138.

(43) Graziani, R.; Bombieri, G.; Forselline, E. *J. Chem. Soc., Dalton Trans.* **1972**, *3*, 2059.

(44) Amara, P.; Field, M. J. Combined Quantum Mechanical and Molecular Mechanical Potentials for the Simulation of Biological Systems. In *The Encyclopedia of Computational Chemistry*, Schleyer, P. v. R., Allinger, N. L., Clark, T., Gasteiger, J., Kollman, P. A., Schaefer, H. F., III, Schreiner, P. R., Ed.; John Wiley and Sons: Chichester, 1998; Vol. 1, p 431.

(45) Rappé, A. K.; Goddard, W. A., III *J. Phys. Chem.* **1991**, *95*, 3358.

(46) Bret, C.; Field, M. J.; Hemmingsen, L. *Mol. Phys.* In press.